

# ULTRALOW EMITTANCE BEAM PRODUCTION BASED ON DOPPLER LASER COOLING AND COUPLING RESONANCE\*

A. Noda<sup>#</sup>, M. Nakao, NIRS, Chiba-city, Japan  
 H. Okamoto, K. Osaki, HU/AdSM, Higashi-Hiroshima, Japan  
 Y. Yuri, JAEA/TARRI, Takasaki, Gunma, Japan  
 H. Souda, Gunma Univ. Maebashi, Gunma, Japan  
 H. Tongu, ICR, Kyoto Univ. Uji-city, Kyoto, Japan  
 K. Jimbo, IAE, Uji-city, Kyoto Japan  
 M. Grieser, MPI-K, Heidelberg, Germany  
 Z. He, FRIB, East Lansing, Michigan USA; TUB, Beijing, China  
 A. Smirnov, JINR, Dubna, Russia

## Abstract

Doppler laser cooling has been applied to low-energy (40 keV)  $^{24}\text{Mg}^+$  ions together with the Synchro-Betatron Resonance Coupling (SBRC) method at the S-LSR in ICR, Kyoto University. The S-LSR storage ring has a high super periodicity of 6 preferable from the beam dynamical point of view. Following the realization of one dimensional (1D) ordering of a 7 MeV proton beam, three dimensional (3D) laser cooling has been experimentally demonstrated for ions with non-negligible velocity ( $v/c=0.0019$ ,  $c$ : light velocity). So as to suppress heating effects due to intra-beam scattering (IBS), the circulating ion beam intensity has been reduced by scraping and the normalized emittances:  $\varepsilon_n$  of  $1.3 \times 10^{-11} \pi \text{ m-rad}$  and  $8.5 \times 10^{-12} \pi \text{ m-rad}$ , corresponding to 6.4 K and 2.1 K, have been realized for the horizontal and vertical directions, respectively with a beam intensity of  $\sim 10^4$ , which are the lowest temperatures ever attained by laser cooling. Molecular Dynamics (MD) computer simulation predicts the realization of the lowest beam temperatures of  $\sim 0.001 \text{ K}$  and  $\sim 0.1 \text{ K}$  corresponding to  $\varepsilon_n$  of the order of  $10^{-13} \pi \text{ m-rad}$  and  $10^{-12} \pi \text{ m-rad}$  for the longitudinal and transverse directions, respectively. With the same condition as utilized for the real experiments at S-LSR, formation of a 1D longitudinal string is expected if the laser spot size and laser detuning are adjusted to the proper values of 1.5 mm and -42 MHz, respectively with ramping of the detuning. 3D ordered state is also predicted for a coasting beam with laser cooling utilizing dispersive cooling.

## INTRODUCTION

Historically, beam cooling was invented from the need of secondary produced beam of anti-proton for the elementary particle physics research, which was finally realized by stochastic cooling [1] more suitable for hot ion beams [2]. Electron cooling invented by G.I. Budker

\*Work supported by Advanced Compact Accelerator Development project by MEXT of Japanese government. It was also supported by GCOE project at Kyoto University, "The next generation of Physics-Spun from Universality and Emergency.

<sup>#</sup>a\_noda@nirs.go.jp

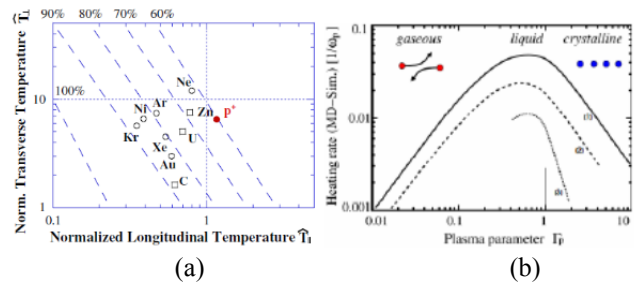


Figure 1: (a) Reflection probabilities of heavy ions at ESR of GSI and S-LSR at ICR. ( $\circ$  and  $\square$  are borrowed from Refs. [4], [7], respectively and data  $\bullet$  are taken at S-LSR [8].) The contour plots of the reflection probabilities are taken from Ref. [9].), (b) Plasma Parameter,  $\Gamma_p$ , dependence of Heating ratio [10], where  $\Gamma_p$  is defined as

$$\Gamma_p = \frac{E_{Coulomb}}{E_{thermal}} = \frac{q^2 e^2}{4\pi\epsilon_0 a_{WS} k_B T_{ion}}, \text{ with } a_{WS} = \left(\frac{4\pi}{3} n_{ion}\right)^{-\frac{1}{3}},$$

where  $a_{WS}$ ,  $q$  and  $n_{ion}$  are Wigner Seitz radius, charge state and 3 dimensional density of the ion beam, respectively.

[3] for the same purpose is more appropriate for cooling of colder ion beams and has been utilized for various precision measurements.

Following the realization of 1D ordered states with an electron cooling for heavy ions at ESR and SIS in GSI and CRYRING in Stockholm [4,5,6], a 7 MeV proton beam having the smallest charge state, was electron cooled to the 1D ordered state at S-LSR by reducing the particle number to  $\sim 2000$  for the first time for single charged ions (Fig. 1(a)) [8]. In these cases, adjacent ions cannot take over each other but be repulsed back just before collision being aligned in a line with distance oscillation, which is different from the crystalline state.

The lattice of S-LSR is designed to suppress beam blow up, satisfying the so called maintenance conditions [11],

$$\gamma \leq \gamma_t \quad (1)$$

$$N_{sp} \geq 2\sqrt{v_H^2 + v_V^2} \quad (2).$$

Thus the S-LSR ring has been designed to have a rather high super-periodicity of 6 [12]. The above mentioned 1D ordered state is based on such characteristics of S-LSR.

For crossing the hill of the heating rate shown in Fig. 1(b) with much stronger cooling force, laser cooling established by Steven Chu, Claude Cohen-Tannoudji and William D. Phillips for trap atoms [13] was also applied for ion beams circulating in a storage ring although the applicable ion species have been limited to  ${}^7\text{Li}^+$  (metastable),  ${}^9\text{Be}^+$ ,  ${}^{24}\text{Mg}^+$  and  ${}^{12}\text{C}^{3+}$  (only with high  $\beta \sim 0.5$ ) due to the limitation of available lasers with an appropriate wavelength and enough power. A further restriction of laser cooling is the one dimensional direction of the cooling force, oriented to the laser beam direction. This limitation has been tried to be removed by various schemes.

In the present paper, the historical approaches in Doppler laser cooling of a circulating ion beam are briefly given and then our attainment at S-LSR utilizing an active 3D laser cooling by SBRC is presented. Finally, our experimental approach to realize a crystalline structure is discussed in connection with the recent results of MD simulations.

## DOPPLER LASER COOLING APPLIED FOR MOVING ION BEAMS (HISTORY)

### Passive 3 D Laser Cooling Scheme

The temperature of the ion beam circulating in a ring, representing the distribution of the velocity of the beam particles in the centre of mass frame and is defined as:

$$k_B T_{\parallel} = m_0 c^2 \beta^2 \left( \frac{\delta p}{p} \right)^2 \quad (3)$$

$$T_y = \frac{1}{k_B} m c^2 \beta^2 \langle \gamma \rangle \frac{\sigma_y^2}{\beta_y} \quad \langle \gamma \rangle = \frac{1}{c_0} \oint \beta^{1+\alpha^2} ds \quad (4)$$

can be reduced with a much stronger laser cooling force, where  $k_B$ ,  $m$ ,  $\beta$ ,  $\sigma_y$  and  $\beta_y$  are Boltzmann constant, ion mass, the ratio of ion velocity to light velocity, beam size and beta-function in y-direction at the point of observation, respectively. It has been applied to various ion beams starting from the first experiment at TSR [14], which, however, was limited only in the longitudinal direction. The extension of the laser cooling to the transverse directions with the use of IBS was performed by H.J. Miesner et al. also at the TSR [15], however the equilibrium temperatures were limited at rather high values of 4000 K and 500 K for the horizontal and

vertical directions, respectively due to the passive scheme of heat exchange among the degrees of freedom. By application of position shifted lasers from the ion beam orbit in parallel at the cooling section (dispersive cooling), the equilibrium temperature could be somewhat reduced to  $\sim 500$  K and  $\sim 150$  K for the horizontal and vertical directions, respectively at the TSR [16]. With the IBS cooling scheme, transverse temperatures down to  $\sim 20$  K could be obtained at ASTRID in Aarhus [17] for an ion beam number of  $7 \times 10^6$  and kinetic energy of 100 keV. The attained temperatures are still not sufficient to realize the crystalline state. The lowest obtained temperatures reported in Ref. [17] results in  $\Gamma_p \sim 0.04$ , far below the heat rate peak shown in Fig. 1(b).

### Active 3 D Laser Cooling Scheme

The SBRC scheme proposed by H. Okamoto, A. Sessler and D. Möhl [18] uses a coupling between the longitudinal and the horizontal degrees of freedom under the condition

$$\nu_H - \nu_s = \text{integer}, \quad (5)$$

while it assumes the coupling between the horizontal and the vertical directions with a solenoid or a skew quadrupole magnet under the condition of

$$\nu_H - \nu_V = \text{integer}, \quad (6)$$

where  $\nu_H$ ,  $\nu_V$  and  $\nu_s$  are the horizontal, vertical and the longitudinal tunes, respectively. This active scheme is expected to attain more efficient cooling force and MD computer simulation predicted a crystalline beam for an ideal system [19, 20] and for the S-LSR lattice with a  ${}^{24}\text{Mg}^+$  beam of the energy 35 keV [21].

## DOPPLER LASER COOLING AT S-LSR TOWARD LOW ION TEMPERATURE

### Laser Cooling at S-LSR with Coasting Beam

At first, laser cooling at S-LSR was applied for a coasting beam using counter deceleration with an induction accelerator [22]. The block diagram of the laser cooling system is illustrated in Fig. 2. The laser light with the wavelength of 280 nm, the output of a ring dye laser pumped with a solid state green laser of the wavelength 532 nm, is doubled in its frequency by a second harmonics generator, is co-propagated with the  ${}^{24}\text{Mg}^+$  ion beam. The direction of the laser beam as well as the  $\text{Mg}^+$  ion beam is defined by two apertures in the cooling section (Fig. 2) of different sizes ( $2\text{mm}^{\phi}$  for laser) and (firstly  $10\text{mm}^{\phi}$  and later  $6\text{mm}^{\phi}$  for the ion beam). The laser photon excites the transition from  $3s^2S_{1/2}$  to  $3p^2P_{3/2}$ .

The momentum spread of the circulating ion beam was observed utilizing the Post Acceleration Tube (PAT) developed at TSR [23] and ASTRID [24]. The longitudinal temperature had reached 3.6 K for  $3 \times 10^4$  40 keV  ${}^{24}\text{Mg}^+$  ions, which was limited as cooling was only efficient in the longitudinal direction and the IBS heating was not negligible with the beam intensity attainable enough S/N ratio for optical observation by PAT.

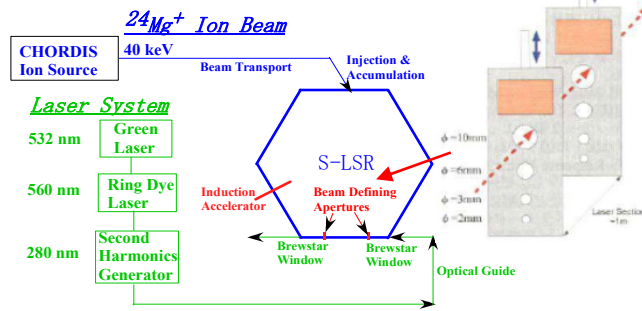


Figure 2: Block diagram of the laser cooling system at S-LSR.

Content from this work may be used under the terms of the CC BY 3.0 licence (© 2014). Any distribution of this work must maintain attribution to the author(s), title of the work, publisher, and DOI.

### Active 3 D Laser Cooling for Bunch Beam

The SBRC scheme has been experimentally applied at S-LSR. With a drift tube cavity, located at a straight section with finite dispersion (~1m), two period downstream from the laser cooling section (Fig. 3), the RF voltage was applied to the ion beam. The 40 keV  $^{24}\text{Mg}^+$  ion beam directly coming from the CHORDIS ion source, without further acceleration, was single turn injected into the ring of S-LSR and captured into a separatrix with an RF voltage as shown in Fig. 4(a). The laser detuning was optimized to minimize the captured bunch length as illustrated in Fig. 4(b).

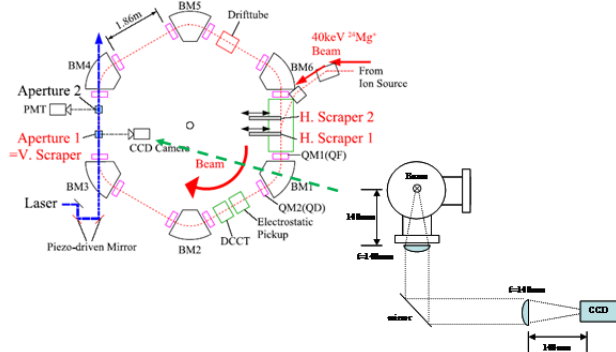


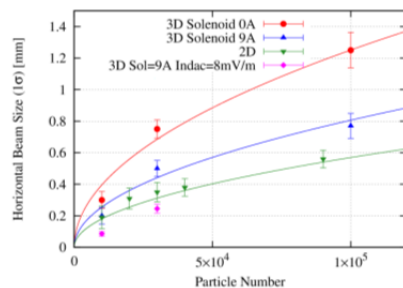
Figure 3: Layout of the Doppler laser cooling system and beam size observation system with a CCD and scrapers [25, 26]. Inlet of the figure shows the optical system using a CCD camera. The distances from the beam and CCD camera to the nearby lenses are set to their focal lengths (140 mm) and the image size is the same as the beam dimension.

## OBSERVATION OF TRANSVERSE TEMPERATURE

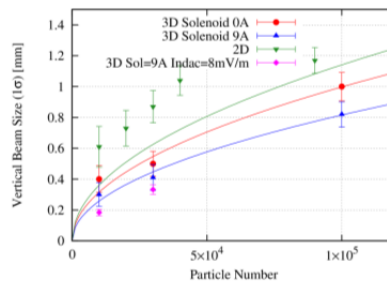
### Optical Measurement by Cooled CCD

Evaluation of the transverse laser cooling effect needs the transverse beam size measurement and the horizontal beam size was observed with a CCD camera cooled down to  $\sim -30^\circ\text{C}$ , followed with an optical system shown in Fig. 3.

SBRC has been attained at the operating point of (2.068, 1.105) at first for 2D coupling between the longitudinal and horizontal degrees of freedom under the condition satisfying only Eq. (5) for a beam intensity larger than  $10^7$



(a) Horizontal beam size



(b) Vertical beam size

Figure 6: Comparison of beam sizes among, 2D, 3D laser cooling with solenoid on and off and additional deceleration by an induction accelerator.

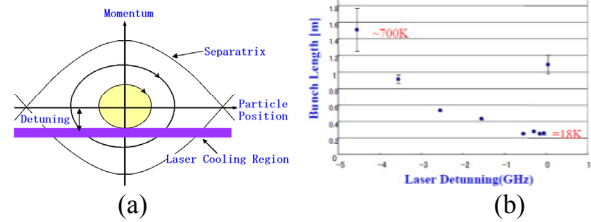


Figure 4: (a) Longitudinal phase space and a detuned laser. (b) Optimization of the laser detuning.

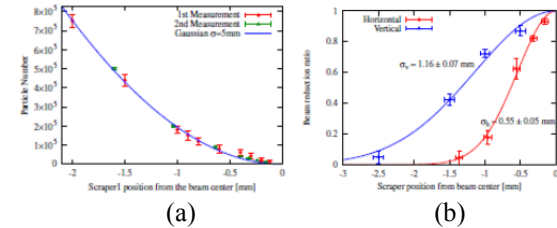


Figure 5: (a) Correlation between the position of the scraper 1 and the survival circulating ion beam intensity in a ring of S-LSR. (b) Typical examples of beam sizes measurements of the horizontal and vertical directions taken at the ion beam intensity of  $9 \times 10^4$  ions [26].

which attains enough S/N ratio for optical observation [25]. With this rather higher ion beam intensity, however, the beam temperature became equilibrium at rather higher level as  $\sim 200$  K (corresponds to:  $\epsilon_n$  of  $\sim 4 \times 10^{-10}$   $\pi$  m·rad) due to heating by IBS [25].

### Beam Size Measurement by Scraping

Increase of the overall laser cooling efficiency in all three dimensions, requires further reduction of the ion utilized optical system, we have established a new beam

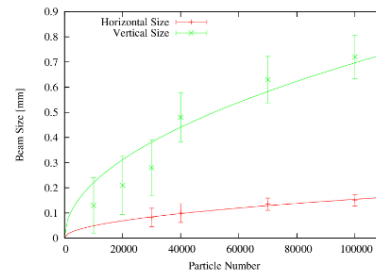


Figure 7: Transversely laser cooled ion beam sizes by SBRC together with deceleration by INDAC.

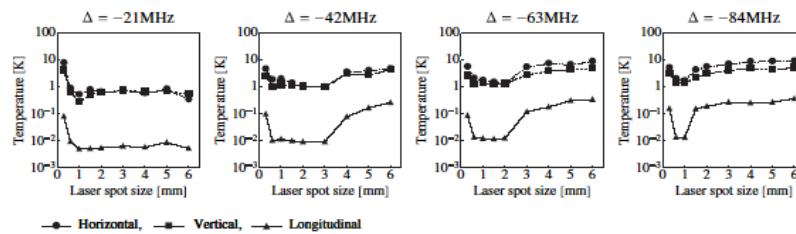


Figure 8: MD simulated 3D laser cooled ion beam temperature [30].

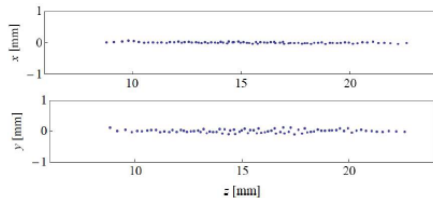


Figure 9: Predicted longitudinal ordered state from MD simulation assuming  $\Delta = -42$  MHz and laser spot size of 1.5 mm (corresponds to the left part of Fig. 10 (b) of Ref. [30])

scraping scheme for evaluation of the transverse beam sizes. After defining the circulating ion beam intensity with the use of H Scraper 1 (Fig. 5(a)), the horizontal or vertical beam size was obtained by observing the survival beam intensities for various positions of H Scraper 2 or V Scraper, respectively as illustrated in Fig. 5 (b) [26]. Suppression of IBS by reducing the beam intensity to  $10^4$  with this scheme, resulted in the equilibrium beam temperature of 20 K and 29 K (corresponding to  $\epsilon_n$  of  $7.0 \times 10^{-10} \pi \text{ m-rad}$   $1.9 \times 10^{-10} \pi \text{ m-rad}$ ) for the horizontal and vertical directions, respectively for the condition of Eq. (5) with the operation point of (2.072, 1.120) [26].

Further we applied 3D laser cooling moving the operation point to (2.067, 1.070) satisfying Eq. (6) together with Eq. (5) for the coupling among the longitudinal, horizontal and vertical freedoms. In Fig. 6, the attained transverse beam sizes in the (a) horizontal and (b) vertical directions are shown for various conditions. The horizontal and vertical coupling was found to be optimum for the solenoid field of 22.5 Gauss at the electron cooler section, which was found to be different from the simulation as is described later. With such coupling, the vertical beam size was reduced

Table 1: Main Parameters of Active 3 D Laser Cooling at S-LSR

Betatron Tune	(2.067, 1.070)
Synchrotron Tune	0.072
Initial Ion Number	$3 \times 10^7$ (scrapped to $1 \times 10^4 - 1 \times 10^5$ )
Initial Momentum Spread	$7 \times 10^{-4}$
Revolution Frequency	25.1735 kHz
RF Frequency	2.51735 MHz ( $h=100$ )
Solenoid Field	22.5 Gauss
Laser Spot Size	$\sigma = 0.30 \text{ mm}$
Laser Power	$8 \pm 1 \text{ mW}$
Average Vacuum Pressure	$9.5 \times 10^{-9} \text{ Pa}$
Indac Voltage	6 mV/m (deceleration)

drastically, while the horizontal beam size gets worse by heat transfer from the vertical direction. The cooled equilibrium beam sizes were 0.20 mm and 0.30 mm for the horizontal and vertical directions, respectively, converted to ring averaged temperatures  $T_H$  and  $T_V$  of 40 K and 11 K, respectively [27].

Further study was performed with deceleration by an induction accelerator in order to give a counter force against ion beam acceleration due to laser photon absorption at every turn. With a laser detuning of -190 MHz, the transverse beam sizes were reduced to 0.09 mm and 0.18 mm for the horizontal and the vertical directions, respectively at an ion beam intensity of  $10^4$ , which corresponded to 8.1 K and 4.1 K (both correspond to  $\epsilon_n$  of  $1.3 \times 10^{-11} \pi \text{ m-rad}$ ). In this case, the laser power was  $\sim 15 \text{ mW}$  at the most optimum condition [27].

Further, the laser detuning was optimized and a detuning of -26 MHz resulted in the lowest beam temperature, which was a little different from the optimum one suggested by the simulation as described later. In that case, the horizontal beam size was measured with a cooled CCD after optimization of the laser size at the position where the horizontal beta-function was 0.89 m. The main parameters of this experiment are listed up in Table 1. The horizontal beam size could be measured only for an ion beam intensity larger than  $3 \times 10^4$  to get the needed S/N ratio. The reason why we can now observe much lower intensity beams with our optical system compared with the previous observation, is that the beam density increased by the application of transverse laser cooling.

At an intensity of  $3 \times 10^4$  ions, the horizontal beam size could be reduced to 0.08 mm and with vertical scraping, 0.13 mm was obtained for an ion number of  $10^4$ . These results correspond to the horizontal and vertical average beam temperatures of 6.4 K and 2.1 K, respectively (Fig. 7), corresponding to  $\epsilon_n$  of  $1.3 \times 10^{-11} \pi \text{ m-rad}$  and  $8.5 \times 10^{-12} \pi \text{ m-rad}$ , respectively [27]. They are already far below the ones of any regular beams except for the one at circular trap with a very low velocity [28], but are not enough cold to reach the crystalline state.

## EXPERIMENTAL ATTAINMENT AND FUTURE PROSPECT BY SIMULATION

The experimental approaches above mentioned, have been simulated with the use of a MD simulation code “CRYSTAL” [29], taking into account the dissipative force induced by a laser photons.

## Bunched Beam 3D Doppler Laser Cooling with SBRC

The recent simulation, changing the laser spot size (defined as the size of the laser waist at the center of the cooling section) from 0.3mm to 6 mm gives the result as shown in Fig. 8 [30]. It shows us we had better to choose the laser spot size a little larger around 1.5 mm instead of our real experimental value of 0.3 mm in March last year. It also gives an optimized field value of the solenoid magnet as 65 Gauss for H-V coupling, which differs from our experimental one (22.5 G), the reasons of which are to be investigated. The MD simulation assuming the same laser power and operation point, but changing only laser spot size and the laser detuning,  $\Delta$ , to 1.5 mm and -42 MHz, respectively with RF voltage ramping in time, predicts realization of longitudinal ordered state (1D string) aligned in a longitudinal direction without oscillation composed of 78 ions in a single bunch as shown in Fig. 9 [30], where the beam temperatures are 0.001K and 0.1K (corresponds to  $\epsilon_n$  of  $10^{-13}$  and  $10^{-12}$   $\pi$ m-rad), for the longitudinal and transverse degrees of freedom, respectively. This is an important step to reach our experimental goal at S-LSR to realize a crystalline string.

## Dispersive Cooling of Coasting Beam

For a coasting beam circulating in the S-LSR ring, Y. Yuri predicted formation of a 3D ordered state with a MD simulation [31] assuming usage of coupling between the

horizontal and longitudinal degrees of freedom by dispersive laser cooling described in Ref. [16]. The estimated temperature is a little bit higher compared with the above simulation for a bunched beam with SBRC [30] due to  $\sim 7$  times larger beam density. With such a condition as a laser spot size ( $1\sigma$ ), laser displacement from the ion beam orbit and a final laser detuning are 2.5 mm, 3 mm and -61 MHz, respectively, the lowest temperature of a coasting beam and hence creation of 3D ordered state is predicted for the ion beam intensity of  $9 \times 10^5$  at the operation point of (1.44, 1.44) as shown in Fig. 10. The betatron tunes are suppressed to 1.20 in the equilibrium due to the space-charge force. In the present case, the phase-space configuration of the ordered beam is hexagonal as shown in Fig. 10(c) different from the case of the crystalline beam of linear configuration [21]. 3D ordered state was reported by Kjærgaard and Drewsen for an ion trap [32, 33], but it is predicted for an ion beam circulating in a ring with a certain velocity for the first time [31].

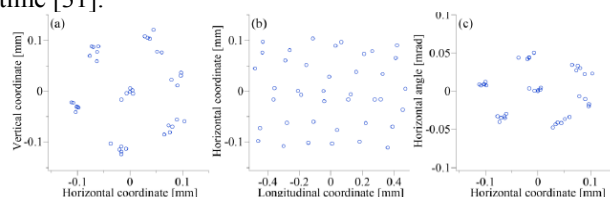


Figure 10: Real space and phase space configurations of the created 3D ordered state by 3D laser cooling combining SBRC with the dispersive cooling [31].

Table 2: Comparison of Laser Cooled Ion Beam Temperatures (Shaded Columns Represent the Recent MD Simulations)

Year Ring	Method	Ion	Kinetic Energy	Intensity	Beam Density	$T_{\parallel}$ (K)	$T_{\perp}$ (K)	$T_V$ (K)	Ref.
1996 TSR	IBS	$^9\text{Be}^+$	7.3 MeV	$2.0 \times 10^7$	$3.6 \times 10^5$	15	4000	500	[15]
1998 TSR	Dispersive cooling	$^9\text{Be}^+$	7.3 MeV	$1.0 \times 10^7$	$1.8 \times 10^5$	few tens	$\sim 500^{\#}$	$\sim 150^{\#}$	[16]
1999 ASTRID	IBS	$^{24}\text{Mg}^+$	100 keV	$7 \times 10^6$	$1.8 \times 10^5$	2-5	17	21	[17]
2001 PALLAS	RFQ	$^{24}\text{Mg}^+$	1 eV	$1.8 \times 10^4$	$5.0 \times 10^4$	$< 0.003$	$T_{\perp} < 0.4$		[28]
2008 S-LSR	IBS	$^{24}\text{Mg}^+$	40 keV	$1.0 \times 10^7$	$4.4 \times 10^5$	11	-	500	[22]
2009 S-LSR	W SBRC (2D)	$^{24}\text{Mg}^+$	40 keV	$1.0 \times 10^7$	$4.4 \times 10^5$	27	220 $^{\$}$		[25]
2009 S-LSR	WO SBRC	$^{24}\text{Mg}^+$	40 keV	$1.0 \times 10^7$	$4.4 \times 10^5$	16			[25]
2012 S-LSR	W SBRC (2D)	$^{24}\text{Mg}^+$	40 keV	$1 \times 10^4$	$4.4 \times 10^2$	(0.4)	20	29	[26]
2013.2.1 S-LSR	W SBRC (3D)	$^{24}\text{Mg}^+$	40 keV	$1 \times 10^4$	$4.4 \times 10^2$	-	40	11	[27]
2013.3.7 S-LSR ( $\Delta f = -190$ MHz)	W SBRC (3D) (INDAC ON)	$^{24}\text{Mg}^+$	40 keV	$1 \times 10^4$	$4.4 \times 10^2$	-	8.1	4.1	[27]
2013.3.22 S-LSR ( $\Delta f = -26$ MHz)	W SBRC (3D) (INDAC ON)	$^{24}\text{Mg}^+$	40 keV	$1 \times 10^4$	$4.4 \times 10^2$	-	6.4 ( $3 \times 10^4$ )	2.1	[27]
Simulation with MD ( $\Delta f = -42$ MHz)	W.SBRC (3D) (RF ramping)	$^{24}\text{Mg}^+$	40 keV	$7.8 \times 10^3$	$6 \times 10^3$	$\sim 0.001$	$\sim 0.1$	$\sim 0.1$	[30]
Simulation with MD ( $\Delta f = -61$ MHz)	W.SBRC (3D) (W Dispersive cooling)	$^{24}\text{Mg}^+$	40 keV	$9 \times 10^5$	$4.0 \times 10^4$	0.003	0.6	0.6	[31]

Content from this work may be used under the terms of the CC BY 3.0 licence (© 2014). Any distribution of this work must maintain attribution to the author(s), title of the work, publisher, and DOI.

## REFERENCES

- [1] S. van der Meer, *Rev. Mod. Phys.*, **57**, 689 (1985).  
[2] D. Möhl, *Proc. ECOOL84*, Karlsruhe, Germany, pp293-301 (1984).  
[3] G. I. Budker, *Proc. Int.Sym.Electron and Positron Storage Rings*, Salay, France, (1966), p II-1-1.  
[4] M. Steck et al., *Phys. Rev. Lett.*, **77**, 3803 (1996).  
[5] M. Steck et al., *Nucl. Instrum. Methods Phys. Res.*, **A532**, 357 (2004).  
[6] H. Danared et al., *J. Phys. B: At. Mol. Opt. Phys.* **36** (2003)1003–1010.  
[7] R.W. Hasse, *Nucl. Instrum. Methods. Phys. Res.* **A532**, 382 (2004).  
[8] T. Shirai et al., *Phys. Rev. Lett.* **98**, 204801 (2007).  
[9] H. Okamoto et al., *Phys. Rev.* **E69**, (2004), 066504.  
[10] M. Bussmann et al., Presentation at SPARC07.  
[11] J. Wei, H. Okamoto and A.M. Sessler, *Phys. Rev. Lett.* **80**, 2606 (1998).  
[12] A. Noda, *Nucl. Instrum. Methods A*, **532** 150 (2004).  
[13] [http://www.nobelprize.org/nobel\\_prizes/physics/laureates/1997/press.html](http://www.nobelprize.org/nobel_prizes/physics/laureates/1997/press.html)  
[14] S. Schröder et al., *Phys. Rev. Lett.* **64**, (1990), 2901.  
[15] H.-J. Miesner et al. *Nucl. Instrm. Methods* **A393** (1996), 634 and H.-J. Miesner et al., *Phys. Rev. Lett.* **77**, (1996), 623.  
[16] I. Lauer et al., *Phys. Rev. Lett.* **81**, 2052 (1998).  
[17] N. Madsen et al., *Phys. Rev. Lett.* **83**, 4301 (1999).  
[18] H. Okamoto, A.M. Sessler and D. Möhl, *Phys. Rev. Lett.* **72**, (1994), 397.  
[19] J.P. Schiffer and P. Kinle, *Z. Phys.* **A321**,181 (1985).  
[20] A. Rahman and J.P. Schiffer, *Phys. Rev. Lett.* **57**, 1133 (1986).  
[21] Y. Yuri and H. Okamoto, *Phys. Rev. ST-AB*, **8**, 114201 (2005).  
[22] M. Tanabe et al., *Applied Physics Express*, **1** (2008) 028001.  
[23] W. Petrich et al., *Phys. Rev.* **A48**, 2127 (1993).  
[24] J.S. Hangst *et al.*, *Phys. Rev. Letts.* **74**, 86 (1995).  
[25] M. Nakao et al., *PR ST-AB*, **15**, (2012), 110102.  
[26] H. Souda et al., *Jpn. J. Appl. Phys.* **52**, 030202 (2013).  
[27] H. Souda, Doctor Thesis, Kyoto University (2013) and A. Noda et al., *Proc. COOL13*, Murren, Switzerland, (2013).  
[28] T. Schätz, U. Schramm and D. Habs, *Nature*, **412** (2001) 717.  
[29] Y. Yuri and H. Okamoto, *Phys. Rev. Lett.* **93**, 204801 (2004).  
[30] K. Osaki and H. Okamoto, *Prog. Theor. Exp. Phys.*, 053G01, (2014).  
[31] Y. Yuri, *JPS Conf. Proc.* **1**, 013014 (2014).  
[32] N. Kjærgaard and M. Drewsen, *Phys. Rev. Lett.*, **91**, 095002 (2003).  
[33] M. Drewsen et al., *Nucl. Instrm. Methods Phys. Res.*, **A532**, pp237-240, (2004) .